23rd ABCM International Congress of Mechanical Engineering
December 6-11, 2015, Rio de Janeiro, RJ, Brazil

PERFORMANCE EVALUATION OF A SENSOR FUSION ALGORITHM FOR ATTITUDE ESTIMATION USING COMMERCIAL IMU AND SCALE STEWART PLATFORM

Marcos Soares Moura Costa[1]
Marco Antonio Meggiolaro[2]
Mauro Speranza Neto[3]
Allan Nogueira de Albuquerque[4]
Marília Maurell Assad[5]
Pontifícia Universidade Católica do Rio de Janeiro – Department of Mechanical Engineering, Control Development Laboratory. Rua Marquês de São Vicente, 225, Gávea, CEP 22451-900, Rio de Janeiro, RJ.
[1]marcos-mcosta@hotmail.com, [2]meggi@puc-rio.br, [3]msn@puc-rio.br, [4]allan@puc-rio.br, [5]mariliamaurell@gmail.com.

Abstract. *IMU (Inertial Measurement Unit) is a set of inertial sensors normally composed of a triaxial accelerometer, a triaxial gyro and a triaxial magnetometer and is widely used in vehicles to evaluate their kinematic states (accelerations, velocities, positions and orientations). These sensors are indispensable in the control of Unmanned Aerial Vehicles (UAV), for example, and, with the recent popularization of these vehicles, there is a great effort in the development and price reduction of these units. In this work, a new sensor fusion algorithm is proposed to improve the estimated attitude (orientation) calculated from the data acquired by a low cost commercial IMU. In this algorithm, the measurements made by the gyro sensor are used to update the state transition matrix and, with an integration procedure, form one estimated attitude. In the other hand, the measurements made by the accelerometer and magnetometer are combined to form the second estimated attitude. Both solutions are fused to form an improved solution. For algorithm validation, the unit is coupled to a Stewart platform which in turn reproduces pre-programmed movements so that there is a known reference of the kinematic state of the IMU. With this reference, the calculated platform attitude values are compared with those obtained by the accelerometer combined with magnetometer solution, with those obtained by the gyro integration solution and with those obtained by the proposed fusion algorithm. The results indicate that the proposed algorithm minimizes noise and drift errors.*

Keywords: *Inertial Measurement Unit, Stewart platform, Sensor Fusion, Attitude Estimation.*

1. INTRODUCTION

In the developed algorithm, the accelerometer, magnetometer and gyro data are combined in order to find the object's attitude with minimal error. Accelerometers can measure the earth's gravitational field acting in its three perpendicular axis. In an equivalent way, the magnetometer can measure the earth's magnetic field acting in its axis. With these two measurements, the full body attitude can be calculated. However, since the accelerometer measurements are severally influenced by external accelerations and vibrations and the magnetometer measurements are influenced by external magnetic fields, this estimated attitude will be noisy and only valid when the body is static and away from sources of magnetic fields.

The gyro sensor can also be used to calculate the body attitude. Its data are free from external influences and has small noise. Nevertheless, to do the attitude estimation, the sensor data must be integrated and, because all the calculation is done in the discrete time, this process will create an accumulated error, called drift.

In order to fix the problems associated with the accelerometer and magnetometer solution (noise and external influences) and the gyro solution (drift), both attitude estimations will be fused. The resulting solution will combine the benefits of the individual sensors and will greatly reduce its weak points.

The main attitude representation system will be the quaternions. This representation can be written in vector form, which facilitates the usage of the state space system. In addition, the quaternions are less non-linear than the Euler angles representation. Its drawback is the fact that there are always two possible representations for any given attitude.

A Stewart platform is a parallel mechanism with six degrees of freedom consisting of six limbs with variable lengths that are connected to a fixed base by six spherical joints and to a moving platform by six universal joints. In the experimental part, the IMU was attached to the platform and a series of pre-programmed movements were executed so that the solutions of the three methods could be compared with a reference attitude obtained by the platform sensors.

2. SENSOR FUSION ALGORITHM

Initially, the accelerometer and magnetometer method and the gyro integration method will be descripted. The fused system will take the two methods as inputs and generate an improved result. Further details of the procedures presented in the subsequent sections can be found at Costa (2014).

2.1 Accelerometer and Magnetometer Attitude Solution

Considering a static situation, the accelerometer will measure only the gravitational acceleration, as shown in Eq. (1).

$$\boldsymbol{gv}^1 = \boldsymbol{accelerometer} = \boldsymbol{R}_0^1\, \boldsymbol{gv}^0 = \boldsymbol{R}_0^1 \begin{bmatrix} 0 \\ 0 \\ g \end{bmatrix} \tag{1}$$

In which $\boldsymbol{gv}^0$ is the gravitational vector in the global reference system (0), $\boldsymbol{gv}^1$ is the gravitational vector in the embedded reference system, $\boldsymbol{R}_0^1$ is the rotational matrix from the embedded to the global reference system and g is the local gravity acceleration. Taking the norm of this vector yields a unitary vector that represents the z-axis of the frame 0 represented in the frame 1, as shown in Eq. (2).

$$\boldsymbol{z}_0^1 = \frac{\boldsymbol{gv}^1}{\|\boldsymbol{gv}^1\|} \tag{2}$$

The magnetometer measurements in an environment free of magnetic influences provides a vector, $\boldsymbol{vm}$, that has components in the x and z-axis of the global reference system and those components represent the local earth's magnetic field. In order to create an axis that is orthogonal to $\boldsymbol{z}_0^1$, the projection of $\boldsymbol{vm}$ in $\boldsymbol{z}_0^1$ is rejected from $\boldsymbol{vm}$, as shown in Eq. (3), in which $\tilde{\boldsymbol{x}}_0^1$ is the non-normalized version of the unitary vector representing the x-axis of the frame 0 represented in frame 1.

$$\tilde{\boldsymbol{x}}_0^1 = \boldsymbol{vm} - (\boldsymbol{vm} * \boldsymbol{z}_0^1)\, \boldsymbol{z}_0^1 \quad \rightarrow \quad \boldsymbol{x}_0^1 = \frac{\tilde{\boldsymbol{x}}_0^1}{\|\tilde{\boldsymbol{x}}_0^1\|} \tag{3}$$

After normalizing $\tilde{\boldsymbol{x}}_0^1$, the unitary y-axis can be obtained by the normalized cross-product between $\boldsymbol{x}_0^1$ and $\boldsymbol{z}_0^1$, as shown in Eq. (4).

$$\tilde{\boldsymbol{y}}_0^1 = \boldsymbol{x}_0^1 \times \boldsymbol{z}_0^1 \quad \rightarrow \quad \boldsymbol{y}_0^1 = \frac{\tilde{\boldsymbol{y}}_0^1}{\|\tilde{\boldsymbol{y}}_0^1\|} \tag{4}$$

The Eq. (5) shows how the three orthogonal unitary vectors ($\boldsymbol{x}_0^1$, $\boldsymbol{y}_0^1$ and $\boldsymbol{z}_0^1$) can be used to compose the rotational matrix that changes the representation from the embedded to the global reference system ($\boldsymbol{R}_0^1$).

$$\boldsymbol{R}_0^1 = \left[\ \boldsymbol{x}_0^1 \mid \boldsymbol{y}_0^1 \mid \boldsymbol{z}_0^1\ \right] \tag{5}$$

As a design choice, the object will be considered free of rotations at the initial time. Therefore, the rotational matrix obtained at the discrete time k needs to be post-multiplied by the same matrix calculated at time zero. This operation is shown in Eq. (6).

$$\boldsymbol{R}_{0_k}^1 \coloneqq \boldsymbol{R}_{0_k}^1\, \boldsymbol{R}_i \tag{6}$$

The resulting matrix is transformed to quaternions. The four possible solutions appear in Eq. (7). The criteria for choosing one of these solutions take into consideration the algorithms stability and is shown in Eq. (8). The demonstration of both equations can be found at Diebel (2006).

$$\boldsymbol{q_1}=\frac{1}{2}\begin{bmatrix}\sqrt{1+r_{11}+r_{22}+r_{33}}\\ \frac{r_{23}-r_{32}}{\sqrt{1+r_{11}+r_{22}+r_{33}}}\\ \frac{r_{31}-r_{13}}{\sqrt{1+r_{11}+r_{22}+r_{33}}}\\ \frac{r_{12}-r_{21}}{\sqrt{1+r_{11}+r_{22}+r_{33}}}\end{bmatrix}, \boldsymbol{q_2}=\frac{1}{2}\begin{bmatrix}\frac{r_{23}-r_{32}}{\sqrt{1+r_{11}-r_{22}-r_{33}}}\\ \sqrt{1+r_{11}-r_{22}-r_{33}}\\ \frac{r_{12}+r_{21}}{\sqrt{1+r_{11}-r_{22}-r_{33}}}\\ \frac{r_{31}+r_{13}}{\sqrt{1+r_{11}-r_{22}-r_{33}}}\end{bmatrix}, \boldsymbol{q_3}=\frac{1}{2}\begin{bmatrix}\frac{r_{31}-r_{13}}{\sqrt{1-r_{11}+r_{22}-r_{33}}}\\ \frac{r_{12}+r_{21}}{\sqrt{1-r_{11}+r_{22}-r_{33}}}\\ \sqrt{1-r_{11}+r_{22}-r_{33}}\\ \frac{r_{23}+r_{32}}{\sqrt{1-r_{11}+r_{22}-r_{33}}}\end{bmatrix}, \boldsymbol{q_4}=\frac{1}{2}\begin{bmatrix}\frac{r_{12}-r_{21}}{\sqrt{1-r_{11}-r_{22}+r_{33}}}\\ \frac{r_{31}+r_{13}}{\sqrt{1-r_{11}-r_{22}+r_{33}}}\\ \frac{r_{23}+r_{32}}{\sqrt{1-r_{11}-r_{22}+r_{33}}}\\ \sqrt{1-r_{11}-r_{22}+r_{33}}\end{bmatrix} \tag{7}$$

$$\boldsymbol{q} = \begin{cases} \boldsymbol{q}_1 \;\; if \;\; r_{22} > -r_{33} \;\; \& \;\; r_{11} > -r_{22} \;\; \& \;\; r_{11} > -r_{33} \\ \boldsymbol{q}_2 \;\; if \;\; r_{22} < -r_{33} \;\; \& \;\; r_{11} > r_{22} \;\; \& \;\; r_{11} > r_{33} \\ \boldsymbol{q}_3 \;\; if \;\; r_{22} > r_{33} \;\; \& \;\; r_{11} < r_{22} \;\; \& \;\; r_{11} < -r_{33} \\ \boldsymbol{q}_4 \;\; if \;\; r_{22} < r_{33} \;\; \& \;\; r_{11} < -r_{22} \;\; \& \;\; r_{11} < r_{33} \end{cases} \tag{8}$$

The resulting vector is normalized, as shown in Eq. (9).

$$\boldsymbol{z}_k = \frac{\boldsymbol{q}}{\|\boldsymbol{q}\|} \tag{9}$$

2.2 Gyro Attitude Solution

According to Diebel (2006), the relationship between the unit quaternion vector and its time derivative ($\dot{\boldsymbol{q}}$) involves the angular velocity embedded in the body (ω). This relationship is exposed in Eq. (10).

$$\dot{\boldsymbol{q}} = \frac{1}{2}\begin{bmatrix} 0 & -\omega_1 & -\omega_2 & -\omega_3 \\ \omega_1 & 0 & \omega_3 & -\omega_2 \\ \omega_2 & -\omega_3 & 0 & \omega_1 \\ \omega_3 & \omega_2 & -\omega_1 & 0 \end{bmatrix}\boldsymbol{q} = \frac{1}{2}\,\boldsymbol{W}\,\boldsymbol{q} \tag{10}$$

The same equation in the discrete time can be achieved with the first order Euler method, as shown in Eq. (11).

$$\begin{aligned} \boldsymbol{q}_k &= \boldsymbol{q}_{k-1} + \Delta t \cdot \frac{1}{2}\boldsymbol{W}_k\,\boldsymbol{q}_{k-1} \\ \underbrace{\tilde{\boldsymbol{q}}_k}_{\boldsymbol{x}_k} &= \underbrace{\left(\boldsymbol{I}_{4x4} + \frac{\Delta t}{2}\,\boldsymbol{W}_k\right)}_{\boldsymbol{A}_k}\underbrace{\boldsymbol{q}_{k-1}}_{\boldsymbol{x}_{k-1}} \end{aligned} \tag{11}$$

The resulting quaternion ($\tilde{\boldsymbol{q}}$) is normalized with Eq. (9).

2.3 Fused Attitude Solution

First, the signs of all the quaternions in both solutions are compared, because equal quaternions vectors with different signs represent the same rotation. The function in Eq. (12) changes the sign of the quaternion vector obtained with the accelerometer and magnetometer solution (defined as $\boldsymbol{z}$) if the majority of the signs in its elements are opposite to the signs at the quaternions obtained with the gyro solution (defined as $\bar{\boldsymbol{x}}$).

$$\boldsymbol{z} = \begin{cases} -\boldsymbol{z}, & \left(\sum_{i=1}^{4}\left(sign(z_i) \neq sign(\bar{x}_i)\right)\right) \geq 2 \\ \boldsymbol{z}, & \left(\sum_{i=1}^{4}\left(sign(z_i) \neq sign(\bar{x}_i)\right)\right) < 2 \end{cases} \tag{12}$$

To fuse both solutions, a simplified and adapted version of the original Kalman filter will be used. The original method can be found at Kalman (1960). The gyro solution, presented in Eq. (11), is used in the prediction step. The mathematic model is considered non-linear, because the state transition matrix ($\boldsymbol{A}_k$) is updated at each time step with new gyro data.

The Quaternion vector calculated with the accelerometer and magnetometer solution is the observation vector ($\boldsymbol{z_k}$) in the method. Consequently, the observation matrix ($\boldsymbol{H}$) is constant and equal to the unit matrix ($\boldsymbol{I_{4x4}}$). The covariance between states will be neglected, so all elements outside the main diagonal in the matrix with the covariance of the process ($\boldsymbol{Q}$) will be considered null. Furthermore, all elements in this matrix will have, by design, the same value, as shown in Eq. (13).

$$\boldsymbol{Q}(\alpha) = \alpha\, \boldsymbol{I}_{4x4}, \qquad \alpha \geq 0 \tag{13}$$

The same criteria are applied to the matrix with the covariance of the observation noise ($\boldsymbol{R}$), as defined in Eq. (14).

$$\boldsymbol{R}(\beta) = \beta\, \boldsymbol{I}_{4x4}, \qquad \beta \geq 0 \tag{14}$$

Alpha (α) and beta (β) parameters will act as weights in the process. Small alphas will give more weight to the gyro solution and small betas will give more weight to the accelerometer and magnetometer solution. These parameters need to be tuned accordingly to the system dynamics and to the sensors used. However, as a general rule, alpha should be two or more orders of magnitude smaller than beta because the gyro solution is much more accurate than the accelerometer and magnetometer solution, has much less noise and is not influenced by external factors. The small weight of the accelerometer and magnetometer solution should be just enough to remove the drift in the gyro solution.

The original Kalman equations are maintained but the simplifications applied to matrices $\boldsymbol{H}$, $\boldsymbol{Q}$ and $\boldsymbol{R}$ will make it loose some of its filtering capabilities. However, since the main goal is to develop a method to fuse two solutions and not to filter undesired noise, the proposed simplified method should be enough to fulfill the task.

3. INVERSE GEOMETRY AND KINEMATICS OF THE STEWART PLATFORM

As shown in the Fig. 1, this mechanism consists of six limbs (with variable lengths d_1, d_2, d_3, d_4, d_5 and d_6) that are connected to a fixed base by six spherical joints (A_1, A_2, A_3, A_4, A_5 and A_6) and to a moving platform by six universal joints (B_1, B_2, B_3, B_4, B_5 and B_6). The position and the orientation of the moving platform are given by x, y, z, φ, θ and ψ.

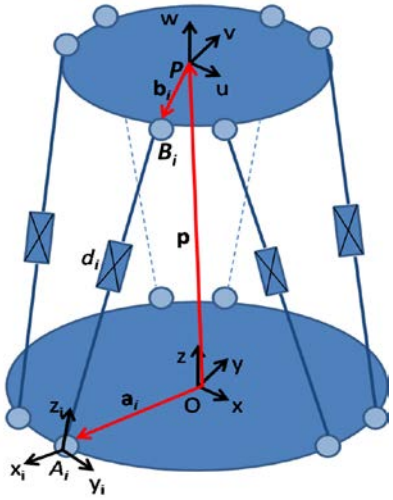

Figure 1. Geometric scheme of a Stewart platform

The inverse geometry could be obtained by the vector sum shown in Eq. (15) with i = 1, …, 6, where $\boldsymbol{R}_B^A$ is the transformation matrix between the fixed frame $A(x, y, z)$ and the moving frame $B(u, v, w)$ (Tsai, L.W., 1999).

$$\overline{A_iB_i} = \overline{OP} + \overline{PB_i} - \overline{OA_i} \;\therefore\; \boldsymbol{d}_i = \boldsymbol{p} + \boldsymbol{R}_B^A\, \boldsymbol{b}_i{}^B - \boldsymbol{a}_i \tag{15}$$

Applying the time derivative in Eq. (15), the Eq. (16) can be obtained. $\boldsymbol{s}_i$ is the unit vector on the direction of the segment $\overline{A_iB_i}$. $\boldsymbol{v}_P$ and $\boldsymbol{\omega}_P$ are the linear and angular speed of the moving platform, respectively, and they form the vector $\dot{\boldsymbol{x}}$, which describes the kinematic state of this platform (Eq. (17)). $\dot{d}_i$, with i = 1, …, 6, are the actuator's linear velocities from the mechanism and they form the vector $\dot{\boldsymbol{q}}$.

$$\dot{d}_i = \boldsymbol{s}_i \cdot \boldsymbol{v}_P + (\boldsymbol{b}_i \times \boldsymbol{s}_i) \cdot \boldsymbol{\omega}_P \tag{16}$$

$$\dot{\boldsymbol{x}} = \begin{bmatrix} \boldsymbol{v}_p \\ \boldsymbol{\omega}_P \end{bmatrix} = \begin{bmatrix} (\dot{x} & \dot{y} & \dot{z})^T \\ (\dot{\phi} & \dot{\theta} & \dot{\psi})^T \end{bmatrix} \tag{17}$$

The inverse Jacobian matrix relates the linear and angular speed of the moving platform ($\dot{\boldsymbol{x}}$) to the linear velocity of the actuators ($\dot{\boldsymbol{q}}$), as shown in Eq. (18).

$$\dot{\boldsymbol{q}} = J^{-1}\dot{\boldsymbol{x}} \tag{18}$$

Separating the variables related to the limbs from the variables related to the moving platform, the inverse jacobian of the mechanism can be written (Eq. (19)). θ_i (with i = 1, …, 6) is the angle between the limb i and the fixed base. b_{iu}, b_{iv} and b_{iw} are the coordinates of the point B_i relative to the frame $B(u, v, w)$. More details about this procedure can be found in Albuquerque (2012).

$$J^{-1} = \begin{bmatrix} c\phi_1 s\theta_1 & s\phi_1 s\theta_1 & c\theta_1 & b_{1v}c\theta_1 - b_{1w}s\phi_1 s\theta_1 & b_{1w}c\phi_1 s\theta_1 - b_{1u}c\theta_1 & b_{1u}s\phi_1 s\theta_1 - b_{1v}c\phi_1 s\theta_1 \\ c\phi_2 s\theta_2 & s\phi_2 s\theta_2 & c\theta_2 & b_{2v}c\theta_2 - b_{2w}s\phi_2 s\theta_2 & b_{2w}c\phi_2 s\theta_2 - b_{2u}c\theta_2 & b_{2u}s\phi_2 s\theta_2 - b_{2v}c\phi_2 s\theta_2 \\ c\phi_3 s\theta_3 & s\phi_3 s\theta_3 & c\theta_3 & b_{3v}c\theta_3 - b_{3w}s\phi_3 s\theta_3 & b_{3w}c\phi_3 s\theta_3 - b_{3u}c\theta_3 & b_{3u}s\phi_3 s\theta_3 - b_{3v}c\phi_3 s\theta_3 \\ c\phi_4 s\theta_4 & s\phi_4 s\theta_4 & c\theta_4 & b_{4v}c\theta_4 - b_{4w}s\phi_4 s\theta_4 & b_{4w}c\phi_4 s\theta_4 - b_{4u}c\theta_4 & b_{4u}s\phi_4 s\theta_4 - b_{4v}c\phi_4 s\theta_4 \\ c\phi_5 s\theta_5 & s\phi_5 s\theta_5 & c\theta_5 & b_{5v}c\theta_5 - b_{5w}s\phi_5 s\theta_5 & b_{5w}c\phi_5 s\theta_5 - b_{5u}c\theta_5 & b_{5u}s\phi_5 s\theta_5 - b_{5v}c\phi_5 s\theta_5 \\ c\phi_6 s\theta_6 & s\phi_6 s\theta_6 & c\theta_6 & b_{6v}c\theta_6 - b_{6w}s\phi_6 s\theta_6 & b_{6w}c\phi_6 s\theta_6 - b_{6u}c\theta_6 & b_{6u}s\phi_6 s\theta_6 - b_{6v}c\phi_6 s\theta_6 \end{bmatrix} \tag{19}$$

4. PERFORMANCE EVALUATION METHOD

For the proposed algorithm validation, the unit is coupled to a Stewart platform with pneumatic actuation which in turn reproduces pre-programmed movements so that there is a known reference of the kinematic state of the IMU. Figure 2 shows different configurations of the Stewart platform.

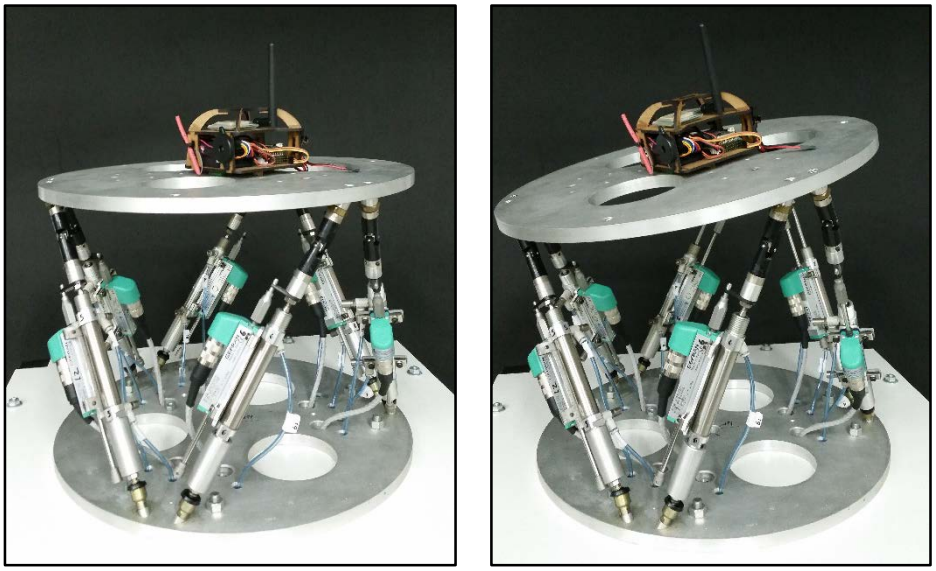

Figure 2. Different configurations of the Stewart platform

The IMU used in this experiment has a tri-axis accelerometer and a triaxial gyro incorporated in one integrated circuit (MPU-6000) and a triaxial magnetometer in another integrated circuit (HMC-5883L). Both circuits are part of the PX4 development platform, commercialized by 3D Robotics.

The alpha and beta parameters were tuned, experimentally, to 0.0001 and 10, respectively. In order to visualize more clearly the results, all obtained quaternions were transformed to Euler Angles (roll, pitch and yaw sequence). This transformation is shown in Eq. (20) and the demonstration can be found at Diebel (2006).

$$\begin{bmatrix}\phi\\ \theta\\ \psi\end{bmatrix}=\begin{bmatrix} tg^{-1}\left(\dfrac{2q_2q_3+2q_0q_1}{q_0^2-q_1^2-q_2^2+q_3^2}\right)\\ -sin^{-1}\left(2q_1q_3-2q_0q_2\right)\\ tg^{-1}\left(\dfrac{2q_1q_2+2q_0q_3}{q_0^2+q_1^2-q_2^2+q_3^2}\right)\end{bmatrix} \tag{20}$$

In this method, the Stewart platform is set to a pre-programmed configuration and the IMU measures the kinematic and geometric state of the moving platform ($\dot{\boldsymbol{x}}_{IMU}$ and $\boldsymbol{x}_{IMU}$). At the same time, the actuators displacements are measured with potentiometric transducers coupled to the pneumatic cylinders and it gives the vector $\boldsymbol{q}_{pot}$. With the IMU data, the vector **x** can be estimated, and, using this to calculate the transducers displacements, another vector $\boldsymbol{q}$ is obtained ($\boldsymbol{q}_{IMU}$). The method of evaluation consists in the comparison between the elements of these two vectors. This is made calculating the Absolute Percentage Error (Eq. (21)) of each actuator (i), at each configuration.

$$APE_i=100\cdot\left|\frac{\boldsymbol{q}_{IMU}(i)-\boldsymbol{q}_{pot}(i)}{\boldsymbol{q}_{pot}(i)}\right| \tag{21}$$

5. RESULTS

The time response of the platform orientation obtained by the IMU using the accelerometer and magnetometer solution, the gyro solution and the fused solution for the pitch angle (θ) can be found in Fig. 3. The first solution shows the undesired noise and the angles that are far from the real ones because of the accelerations involved in the motion. The second solution has much or almost none noise but it drifts apart from the real angles. The fused solution successfully cancels the noise, the drift and is much closer to the real platform attitude.

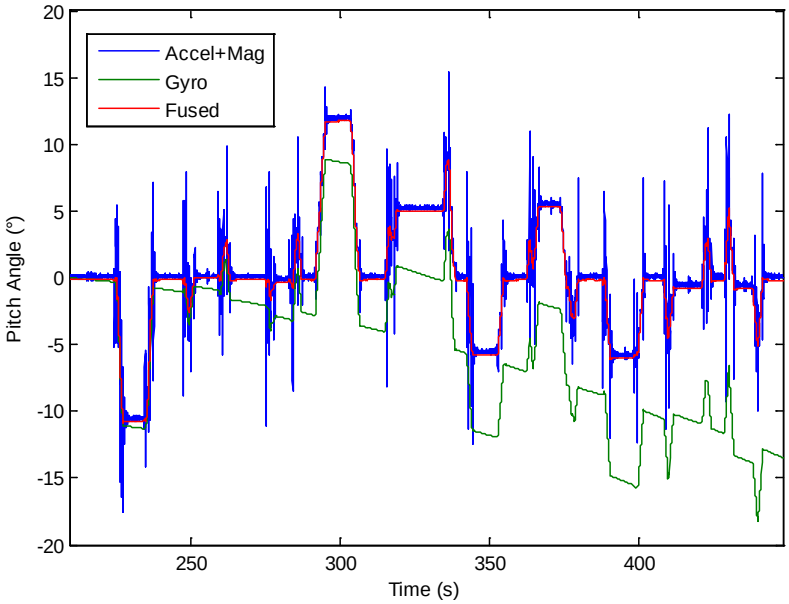

Figure 3. Comparison between the three solutions for the pitch angle (θ)

The time response of the platform orientation obtained by the IMU using the fused solution can be found in Fig. 4. The numbers correspond to each configuration tested and, for each one, the orientation of the platform is concatenated with the known position values (all configurations were chosen with this restriction) and thus, the vector $\boldsymbol{x}_{IMU}$ was created. This vector was transformed in the vector $\boldsymbol{q}_{IMU}$ using the inverse geometry evaluated at each configuration. After this procedure, the vector $\boldsymbol{q}_{IMU}$ is compared with the vector $\boldsymbol{q}_{pot}$ obtained by measuring the displacement of platform actuators. Table 1 shows the Absolute Percentage Error (calculated by Eq. (21)) in each of these configurations.

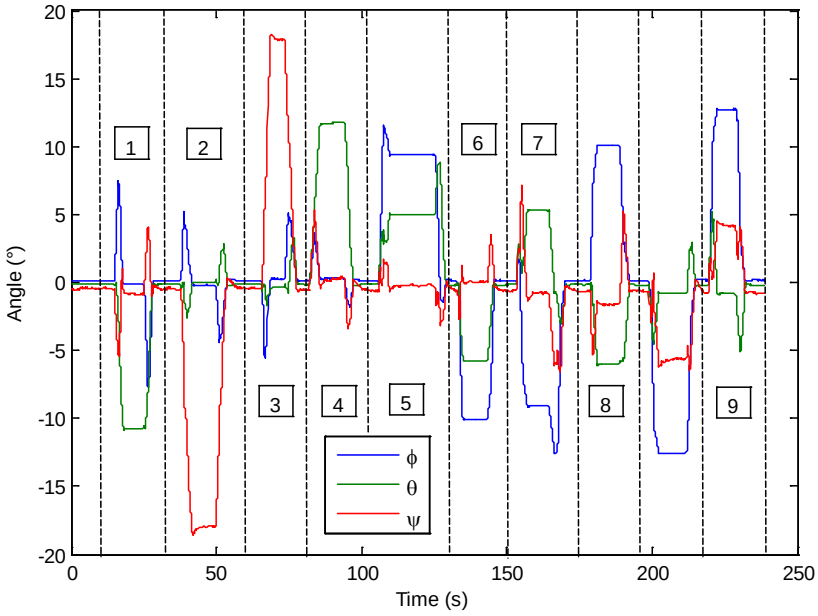

Figure 4. Angles estimated with fused solution in each configuration

Table 1. Absolute percentage error in each configuration.

Configuration	**1**	**2**	**3**	**4**	**5**	**6**	**7**	**8**	**9**
APE_1 (%)	3.4	2.1	2.4	0.8	2.5	1.1	0.4	0.1	0.2
APE_2 (%)	3.5	1.7	1.9	0.1	0.2	1.7	0.9	1.1	0.4
APE_3 (%)	1.7	2.3	1.9	0.1	4.3	0.3	0.2	3.1	1.4
APE_4 (%)	0.5	1.9	2.3	0.7	2.6	0.4	0.8	1.8	0.8
APE_5 (%)	2.9	2.1	1.5	0.5	0.1	0.1	1.1	0.7	0.4
APE_6 (%)	2.2	2.0	1.8	0.6	1.2	0.4	0.4	1.0	0.7

6. CONCLUSIONS AND FUTURE WORK

This work presented solutions for estimating attitude based on inertial sensors measurements, such as accelerometers, gyros and magnetometers. Experimental tests showed that the solutions based on individual measurements of the sensors had poor results. The use of the proposed algorithm made possible to merge the results of sensors and obtain estimates that optimize the measurements of each sensor. Thus, the fused solution have been proposed and validated in experimental tests.

Hence, the comparison between the values obtained by the proposed algorithm and those obtained with the gyro attitude estimation and using the accelerometer and magnetometer attitude estimation shows that the fused algorithm reached small error values when compared to the other methods. This indicates the possibility to use this kind of technique in most types of inertial measurement units.

The evaluation method presented in this paper works only in static configurations of the platform, therefore, the ongoing work focuses on extending the validation method to one in which the time response of the fused solution can be compared with the time response obtained by the inverse kinematics of the Stewart platform. For this, are being evaluated ways to obtain the platform position in real time. After making the dynamic validation of the fused solution, the unit will be attached to the Stewart platform and the control loop described in Albuquerque *et al* (2013) may be implemented. Furthermore, engaging the unit on a quadrotor aerial vehicle, a control strategy such as described in Costa (2014) can also be implemented.

7. ACKNOWLEDGEMENTS

The authors of this work would like to thank FAPERJ for the financial support and the Technological Institute of the Catholic University (ITUC) for the technical support on the manufacturing of the platform.

8. REFERENCES

Albuquerque, A. N., 2012. "Modelagem e simulação de uma plataforma de Stewart controlada usando sensores inerciais", Department of Mechanical Engineering, Pontifical Catholic University of Rio de Janeiro. Master's Dissertation. Rio de Janeiro, Brazil.

Albuquerque, A. N., Speranza Neto, M., Meggiolaro, M. A., 2013. "Parallel mechanisms controlled by non-conventional control strategies", DINAME 2013-Proceedings of the XV International Symposium on Dynamic Problems of Mechanics. ABCM, Buzios, RJ, Brazil.

Costa, M. S. M., 2014. "Controle de veículos aéreos quadrirrotores – Uso de filtros de Kalman para minimização de erros na unidade de medida inercial", Department of Mechanical Engineering, Pontifical Catholic University of Rio de Janeiro. Master's Dissertation. Rio de Janeiro, Brazil.

Diebel, J., 2006. "Representing Attitude: Euler angles, Unit Quaternions, and Rotation Vectors".

Kalman, R. E., 1960. "A new approach to linear filtering and prediction problems", Journal of Fluids Engineering, v. 82, n. 1, p. 35-45. ISSN 0098-2202.

Tsai, L.W., 1999, "Robot analysis – The mechanical of serial and parallel manipulators", Department of Mechanical Engineering and Institute for Systems Research, University of Maryland, USA. John Wiley & Sons, Inc.

9. RESPONSIBILITY NOTICE

The authors are the only responsible for the printed material included in this paper.